ELSEVIER

International Journal of Pharmaceutics 124 (1995) 241–252

international journal of pharmaceutics

Determination of mass transfer coefficients during freeze drying using modeling and parameter estimation techniques

Wei-Youh Kuu *, James McShane, Joseph Wong

Pharmaceutical Sciences R&D, Baxter Healthcare Corporation, Round Lake, IL 60073, USA

Received 2 May 1994; revised 1 February 1995; accepted 17 March 1995

Abstract

An approach using mathematical modeling and parameter estimation techniques was established to determine the best-fit mass transfer coefficients of the dried-layer resistance during primary drying of pharmaceuticals, in order to minimize experimental efforts. For modeling of the primary drying process, the equations associated with heat and mass transfer mechanisms established by Pikal were used as the model equations, whereas the parameter estimation was accomplished by Powell's nonlinear least-squares minimization algorithm. The advantages of this approach include that it can be applied to analyze various types of measurable quantities, such as the cumulative mass of sublimation M_t, the temperature profiles at the bottom center of the frozen layer T_b, and the pressure profiles of the vials. It can also be used for these quantities measured using the vials with different heat transfer coefficients. To test the performance of the proposed approach, hypothetical values of M_t and T_b, with perturbed errors, were simulated using the modeling algorithm and a random number generator. These values were in turn used as the input data for parameter estimation. The results show that the best-fit mass transfer coefficients are successfully obtained using either the hypothetical M_t or T_b profiles, with appropriate initial guesses of the parameters. All computations in modeling and parameter estimation were developed in FORTRAN and compiled using Microsoft FORTRAN compiler, of which the source codes and documentation, with detailed mathematical equations and computation steps, are available upon request.

Keywords: Freeze drying; Collapse temperature; Monte Carlo simulation; Pikal's models; Powell's algorithm; Parameter estimation; Pseudo steady state; Random number generator

1. Introduction

The heat and mass transfer mechanisms involved in the primary drying of pharmaceuticals have been extensively investigated by a number of researchers (Dyer and Sunderland, 1968; Karel, 1975; Mellor, 1978; Ho and Roseman, 1979; Nail, 1980; Pikal et al., 1984; Millman et al., 1985; Pikal, 1985; Lombrana and Diaz, 1987; Jennings, 1988). Among them, one of the most thorough analyses was attributed to Pikal (1985) who combined all processes in the primary drying from the shelf to the condenser. During the course of drying, one of the most important issues is to maintain the sample temperature below the collapse temperature (or eutectic temperature for

* Corresponding author.

SSDI 0378-5173(95)00094-1

compounds that form crystallines after freezing). The sample temperature is not normally directly controlled. Rather, the shelf temperature and chamber pressure are directly controlled, and the product temperature is automatically adjusted according to the balance between heat input from the shelves and heat removed by sublimation. In this sublimation process, the product temperature becomes a function of the sublimation rate, the geometry and configuration of the vial, the thickness of the frozen product in the vial, the chamber pressure, and the mass transfer resistance of the dried layer. The dried-layer resistance is particularly important for a relatively thick solution. It gradually increases during the drying period, resulting in increasing of the mass transfer resistance through the dried layer, followed by warming of the frozen layer. As such, a desired beginning temperature of the frozen layer does not always warrant a successful primary drying throughout the entire period.

The thickness of the solution to be freeze dried is conventionally thin, preferably less than 2.5 cm to avoid prolonged drying time. In addition to the conventional applications of freeze drying, the advantages of freeze drying, such as rapid reconstitution and sterile fill capability, have been found to be very useful in some new pharmaceutical applications, such as controlled drug delivery. In these new applications, the thickness of the product may vary over a wide range in order to meet certain product requirement criteria. For this case, it is important to maintain the temperature profile of the frozen layer below the collapse temperature in the entire primary drying period. Since it is very difficult to perform continual sampling and assays to determine the progress of freeze-drying once the vacuum system is started, mathematical modeling becomes very important for such a complex system. The mathematical modeling can be used to predict optimum drying conditions to ensure that the quality of the products can be maintained.

The objectives of this work include: (1) to develop FORTRAN programs to perform modeling and simulations for the primary drying process; and (2) to evaluate the dried-layer mass transfer coefficients using a parameter estimation technique in order to minimize experimental efforts.

2. Modeling and parameter estimation of primary drying process

2.1. Equations of heat and mass transfer

The primary drying process is governed by the complex heat and mass transfer mechanisms through the vial, as depicted in Fig. 1. To simplify the mechanisms, it is assumed that the heat and mass transfer processes are one-dimensional and vary only in the vertical direction. This may be achieved by thermal shielding from adjacent vials (Pikal et al., 1984) or, for a research purpose, by insulating the side walls of the vials. In Fig. 1, as soon as the thermal equilibrium is established, it is reasonable to assume that a pseudo steady state is established within a small time interval of sublimation. This assumption includes two implications. First, the rate of heat transfer across the various phases, from the shelf to the surface of the frozen layer, is constant. Second, the temperature profile is linear across the frozen layer at any drying time during primary drying.

The equations of heat and mass transfer mechanisms used in this paper are obtained from Pikal (1985, Eq. 2, 3, 15, 18, 22–26, 31, 32, and 41),

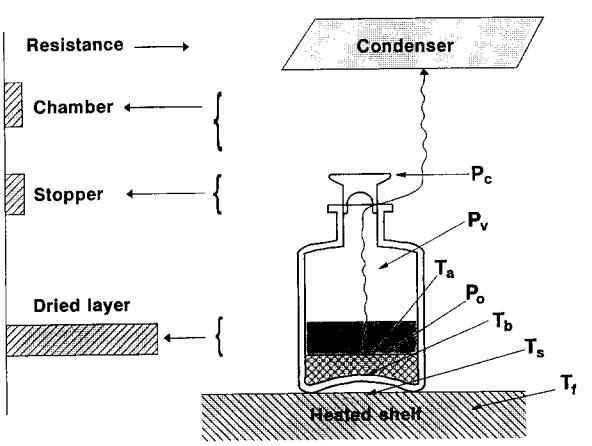

Fig. 1. Schematic diagram of temperature, pressure, and mass transfer resistances, in primary drying.

except that the general empirical equation for evaluating the dried-layer resistance (Eq. 12 in Pikal's paper) is modified to include the effect of temperature. This equation may be expressed in terms of temperature in various forms. In this paper, the following equation is used:

$$\hat{R}_p = \frac{(R_0 + A_1 \ell)(T_a/273)^{A_4}}{1 + A_2 \ell (T_a/273)^{A_3}} \quad (1)$$

where R_0, A_1, A_2, A_3, and A_4 are the mass transfer coefficients; T_a is defined as the temperature at the moving surface of the frozen layer in this paper and ℓ as the thickness of the dried layer at any time. Under an isothermal condition, $\hat{R}_p$ may be directly determined by experiment, such as the microbalance technology used by Pikal et al. (1983), where the dried-layer resistances of a number of formulations under various thermal histories have been obtained using this method. A sophisticated freeze-drying microbalance, however, is needed to perform this task. The approach proposed in this paper intends to minimize the experimental efforts. It will be shown later that the parameter estimation approach proposed in this work does not need to assume an isothermal condition. In the computation procedure, T_a is automatically adjusted by the heat and mass transfer mechanisms. A numerical exercise shows that Eq. 1 gives an excellent fit to the experimental data of potassium chloride and povidone determined at various temperatures, under each isothermal condition, as reported by Pikal et al. (1983). The resulting mass transfer coefficients are given as: $R_0 = 5.351$, $A_1 = 47.67$, $A_2 = 60.18$, $A_3 = 43.12$, $A_4 = 7.109$ for potassium chloride, and $R_0 = 2.86$, $A_1 = 10.89$, $A_2 = 5590.8$, $A_3 = 95.70$, and $A_4 = 6.125$ for povidone.

2.2. Primary-drying subroutine PDRYS

The entire modeling process for the primary drying was developed using FORTRAN and compiled in a primary-drying subroutine PDRYS. The solutions of the simultaneous heat and mass transfer equations were performed by the Newton-Ralphson iteration method (Carnahan et al., 1969, p. 319). For convenience of use, the computations of the primary drying process were developed based on two options, the fixed time interval (FTI) and the fixed thickness interval (FTHI). In the former option, the drying time is treated as the independent variable, whereas the dried-layer thickness becomes one of the dependent variables. This approach is more realistic from experimental design standpoint, since in general drying time is much easier to monitor than the dried-layer thickness. On the other hand, in the later approach the dried-layer thickness is the independent variable, whereas the drying time becomes one of the dependent variables. This option is similar to that in the software package MLAB used by Pikal (1985), where the primary drying was divided into several stages and the mean sublimation rate was evaluated for each stage. Thus, this option was developed primarily for comparison of the approach proposed in this work with that used by Pikal (1985). The entire computation scheme is illustrated by the flow diagram in Fig. 2. The heat and mass transfer equations become simultaneous nonlinear algebraic equations in terms of the six variables $\dot{m}$ (sublimation rate), T_s (shelf temperature), T_t (surface temperature of the tray), T_b (temperature at the bottom center of the frozen layer), T_a (temperature at the moving surface of the frozen layer), and P_v (pressure in the vial). For each incremental time interval or thickness interval under the pseudo steady-state condition, these equations were solved by the Newton-Ralphson iteration method, as described earlier, to obtain the solutions for the six variables.

The dried-layer thickness ℓ for the FTI option or the drying time t (in h) for the FTHI option are then updated for each computation step. The cumulative mass of sublimation for either option is also computed, as described below.

2.2.1. FTI option

The change in the sublimed mass ΔM_t in each computation step for the FTI option is computed by

$$\Delta M_t = \dot{m}_{avg} \Delta t / 60 \quad (2)$$

where $\dot{m}_{avg}$ is the average rate of sublimation in g/h, between two computation steps; the time

interval Δt is in min. The corresponding change in the frozen layer thickness $\Delta \ell$, in cm, is then obtained as:

$$\Delta \ell = \frac{4\Delta M_t}{\pi d^2 \rho_I \epsilon} \tag{3}$$

where ρ_I is the density of ice, which can be found in the literature (Rohsenow et al., 1985) equal to 0.917 g/cm^3 at 0°C; ϵ is the porosity or volume fraction of water in the frozen layer; d is the inside diameter of the vial. Thus, ℓ and M_t become:

$$\ell = \ell + \Delta \ell \tag{4}$$

and

$$M_t = \Sigma \dot{m}_{avg} \Delta t / 60 \tag{5}$$

2.2.2. FTHI option

The change in the drying time Δt in each computation step for the FTHI option is computed by:

$$\Delta t = \frac{\pi d^2 \Delta \ell \rho_I \epsilon 60}{4\dot{m}_{avg}} \tag{6}$$

The corresponding change of the sublimation mass ΔM_t is the same as Eq. 2. Thus, the drying time t and M_t become:

$$t = t + \Delta t / 60 \tag{7}$$

and

$$M_t = \Sigma \dot{m}_{avg} \Delta t / 60 \tag{8}$$

Using the pseudo steady-state approximation described earlier, the procedures described from Eq. 2 to 8 are repeated for both options until ℓ is equal to ℓ_m. For convenience of discussion in the proceeding sections, the region within the dotted lines in Fig. 2 is termed the primary-drying subroutines PDRYS.

2.3. Parameter estimation –using Powell's algorithm

The purpose of parameter estimation in this section is to search for the best-fit dried-layer mass transfer coefficients to the experimental data. In order to perform this task, an iterative, or trial-and-error, computation procedure is employed. For each iteration, if the discrepancy between the experimental and computed data is high, the values of the initial guess of the parameters are adjusted until no further improvement is observed. The foregoing procedure is equivalent to the nonlinear least-squares algorithm, where the best-fit values of the parameters are obtained by minimizing the following sum of the squares, SSQ:

$$\mathrm{SSQ} = \sum_{i=1}^{N} \left[W_i \left(\hat{Y}(t) - Y_i(t) \right) \right]^2 \tag{9}$$

where $\hat{Y}(t)$ and $Y_i(t)$ are the theoretically and experimentally determined dependent variable, respectively, N denotes the number of experimental data points, and W_i is the pertinent weighting factor for each data point. The commonly used values of W_i are 1 and $1/\hat{Y}$. The former indicates that the error variances of the observed dependent variable are constant over

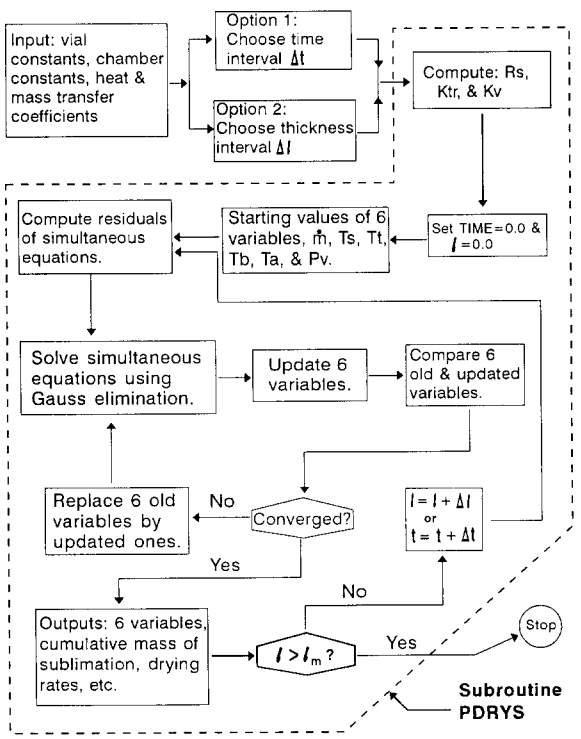

Fig. 2. Computation schemes of the primary drying computer subroutine PDRYS.

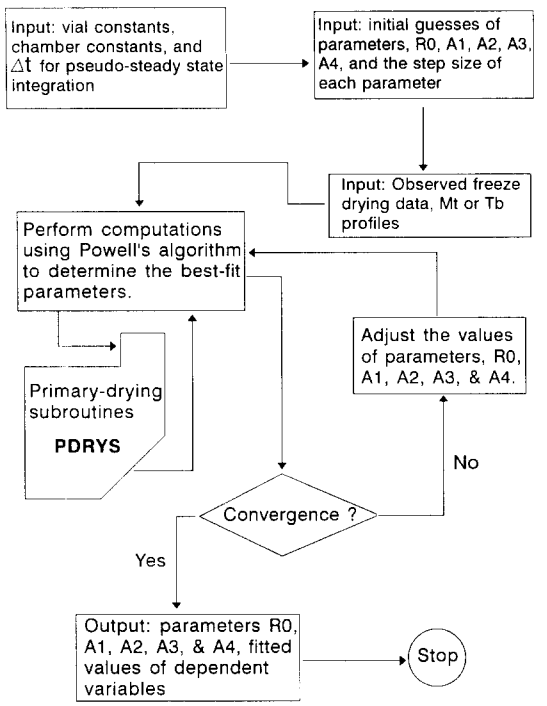

Fig. 3. Computation schemes of the parameter estimation using Powell's algorithm.

the entire range of measurement. The latter indicates that the error variances of the observed dependent variable are proportional to the reciprocals of predicted values of the dependent variable. The nonlinear least-square procedure described by Eq. 9 was performed using Powell's algorithm (Powell, 1965). The advantages of Powell's algorithm have been extensively discussed by Himmelblau (1972), Kuu et al. (1992), and Kuu (1992). Due to the versatility of this algorithm, the parameters can be determined as the 'best-fit' values over the entire time course of the primary drying. The entire computation scheme is illustrated by the flow diagram in Fig. 3.

In the paper by Pikal (1985), it is reported that the software package MLAB was used to solve the simultaneous heat and mass transfer equations. MLAB is a sophisticated commercialized software package designed for general mathematical modeling and parameter estimation purposes, originally developed at the National Institutes of Health for DEC computers, and is now available in enhanced form for IBM PCs and compatible from Civilized Software, Inc. (Bethesda, MD). The major components of the MLAB system include: (1) a curve fitting to determine the parameters of a model function; (2) a differential equation system solving program; and (3) an extensive repertoire of mathematical and statistical functions and operators. It is clear that MLAB is not designed specifically for solving freeze drying problems. By comparison, the primary purpose of this paper for parameter estimation is intended to develop computation schemes which are specifically for solving the primary drying problems described in this paper. The particular problems encountered in this paper are not simple curve-fitting tasks. They include: (1) a nonlinear parameter estimation algorithm with complex objective functions which cannot be expressed in equation forms and have to be developed in computer subroutines; (2) a pseudo steady-state approximation in each incremental time interval or thickness interval; and (3) a non-isothermal dried-layer resistance which consists of a moving surface temperature of the frozen layer that needs to be updated for each computation step. The current version of MLAB appears to have difficulty in performing the tasks described above.

3. Results and discussion

3.1. Comparison with data in the literature

The experimental and simulated data for 5% mannitol and 5% povidone (PVP) reported by Pikal (1985) were used to assess the validity of the primary drying subroutine PDRYS developed in this work. The maximum thickness of the dried layer is 1.3 cm for both formulations. The source codes were compiled using Microsoft FORTRAN compiler version 5.1, and the resulting executable files were run using an IBM compatible personnel computer. The selected outputs for comparison are the cycle time, shelf temperature, mean product temperature, and maximum product temperature. The dried-layer mass transfer coefficients used for computations, as given by Pikal

Table 1
Comparison of simulated data from this work with that reported by Pikal (1985): pilot dryer with vials placed on the shelf without tray lid (NS = 5)

Product	Vial	Fill volume (ml)	Shelf interior (°C)	P_c (mm)	Cycle time (h)	Temperature			Source
						Shelf surface [a]	Mean product [a]	Maximum product	
PVP (Povidone)	W5816	8	−5	0.10	25.8	−9.6	−27.8	−25.3	Pikal [b] (1985)
					26.9	−9.9	−27.3	−24.6	Pikal (1985)
					26.6	−9.6	−26.8	−24.4	this work
Mannitol	W5816	8	−5	0.10	33.4	−8.6	−22.4	−20.2	Pikal [b] (1985)
					34.8	−8.9	−22.9	−18.5	Pikal (1985)
					34.7	−8.5	−21.5	−18.4	this work
Mannitol	W5816	8	+15	0.10	19.2	+6.2	−17.0	−14.2	Pikal [b] (1985)
					19.1	+8.0	−17.0	−11.8	Pikal (1985)
					18.9	+8.6	−15.4	−11.6	this work
Mannitol	W5816	8	+15	0.40	14.0	+5.7	−13.0	−11.9	Pikal [b] (1985)
					15.8	+6.6	−11.8	−8.0	Pikal (1985)
					15.5	+7.2	−10.8	−7.8	this work
Mannitol	5303	20	+15	0.40	19.2	+6.1	−14.5	−12.8	Pikal [b] (1985)
					19.0	+8.1	−13.5	−9.7	Pikal (1985)
					18.8	+8.6	−12.5	−9.5	this work

[a] It is noted that in order to give a more meaningful comparison, the mean shelf surface temperature and the mean product temperature used above are the midpoint temperatures, evaluated at $\ell = \ell_m/2$.
[b] Experimental.

(1985), are: (1) $R_0 = 1.40$, $A_1 = 16.0$, and $A_2 = A_3 = A_4 = 0.0$, for 5% mannitol; and (2) $R_0 = 1.13$, $A_1 = 5.0$, and $A_2 = A_3 = A_4 = 0.0$, for 5% povidone. It is noted that for $A_2 = A_3 = A_4 = 0.0$, Eq. 1 becomes identical to Eq. 12 in the paper by Pikal (1985) for the case of 5% mannitol and 5% povidone. The simulated results by Pikal (1985, Table VI) and those obtained from this work are presented in Table 1, using the same number of drying stages NS for both methods in order to perform a direct comparison. It shows that the results obtained in this work are very close to those obtained by the simulated results by Pikal (1985), and fairly close to those obtained by experiments, indicating the validity of the PDRYS subroutine.

3.2. Parameter estimation –determination of dried-layer resistance

The input data for performing parameter estimation include the measurable independent and dependent variables. The measurable independent variable used here is the drying time. Various measurable dependent variables can be used. They include: (1) the cumulative mass of sublimation M_t, (2) the temperature profile at the bottom center of the frozen layer T_b, (3) the temperature profile at any specific location along the axis of the frozen layer, and (4) the pressure profile in the vial P_v. These variables can be easily generated through the subroutine PDRYS depicted in Fig. 2. In this paper, only the first two dependent variables are discussed. In order to test the proposed parameter estimation approach, two sets of data were generated using PDRYS and used as the hypothetical input data for parameter estimation, as depicted by the computation schemes in Fig. 3. These data sets were chosen to closely mimic two freeze-drying scenarios. The first data set was generated using the vials with constant heat transfer coefficients using the FTI option and the value of Δt was set to 10 min, which was tested to give sufficient accuracy of computations. The values of M_t and T_b were then computed at several time points. The typical vial chosen, as given by Pikal et al. (1984) and Pikal (1985), is 5800W (from Wheaton Glass Co.),

Table 2
Hypothetical and estimated values of M_t and T_b as a function of time, with constant vial heat transfer coefficients

(1) Time (min)	(2) M_{ti} (g)	(3) T_{bi} (K)	(4) $\hat{M}_t$ (g)	(5) $\hat{M}_t$ (g)	(6) $\hat{T}_b$ (K)	(7) $\hat{T}_b$ (K)
60	0.25352	248.732	0.25303	0.25402	248.355	248.886
120	0.48756	250.231	0.48675	0.49019	249.913	250.373
180	0.70981	251.154	0.70866	0.71493	250.879	251.134
240	0.92458	251.759	0.92302	0.93194	251.517	251.580
300	1.13433	252.173	1.13229	1.14343	251.957	251.863
360	1.34059	252.468	1.33798	1.35082	252.271	252.050
420	1.54433	252.684	1.54107	1.55507	252.501	252.177
480	1.74621	252.843	1.74222	1.75688	252.672	252.263
540	1.94670	252.963	1.94193	1.95675	252.800	252.320
600	2.14616	253.053	2.14053	2.15507	252.897	252.357

The values of R_0, A_1, A_2, A_3, A_4, and SSQ for each trial are given by the following parameter sets obtained, indicated by the column number:
(2) Set no. 1, 5.351, 47.67, 60.18, 43.12, 7.109, SSQ = 0.3096×10^{-2} ($W_i = 1/\hat{Y}$).
(3) Set no. 1, 5.351, 47.67, 60.18, 43.12, 7.109, SSQ = 31.44 ($W_i = 1$).
(4) Set no. 2: 6.574, 55.56, 42.63, 39.00, 8.748, SSQ = 0.2982×10^{-2} ($W_i = 1/\hat{Y}$).
(5) Set no. 3: 5.402, 44.38, 9.988, 23.98, 7.109, SSQ = 0.3687×10^{-2} ($W_i = 1/\hat{Y}$).
(6) Set no. 4: 3.484, 35.11, 78.11, 47.39, 4.376, SSQ = 30.09 ($W_i = 1$).
(7) Set no. 5: 2.148, 37.33, 62.72, 35.05, 0.6187, SSQ = 30.97 ($W_i = 1$).
Hypothetical experimental conditions: vial, 5800W; formulation, 8 ml of 5% KCl; ATV = 5.195 cm^2, $A_V = 4.71$ cm^2, $A_p = 3.80$ cm^2, $P_c = 0.1$ mmHg, $K_p = 3.32 \times 10^{-3}$, $T_f = 273.0$ K, KC = 2.64×10^{-4}, KD = 3.64, KTC = 100, KTP = 100, KTD = 1, $K_1 = 0.0059$, $K_S = 0.0015$, $S_0 = 4.8$, $S_1 = 169.0$, $\Delta t = 5$ min, $d = 2.20$ cm, $\rho_1 = 0.917$ g/cm^3, $\epsilon \approx 1 - 0.05 = 0.95$, $\ell_m = 2.3$ cm.

with $A_V = 4.71$ cm^2, and $A_p = 3.80$ cm^2, KC = 2.64×10^{-4}, and KD = 3.64. The formulation chosen was 8 ml of 5% KCl, with the following dried-layer mass transfer coefficients, as described earlier: $R_0 = 5.351$, $A_1 = 47.67$, $A_2 = 60.18$, $A_3 = 43.12$, and $A_4 = 7.109$. The results are listed in Table 2, columns 2 and 3, where the density of the ice used was obtained from Rohsenow et al., as described earlier. Without experimental data and only for modeling purposes, the volume fraction of water ϵ is approximated as (1 − percent of drug concentration/100). The second scenario is the vials with different heat transfer coefficients, hence with different values of KC and KD, so that the drying rate varies from vial to vial. Ideally, with this type of experimental design, various values of the dried-layer thickness may be obtained at one time point. The values of M_t and T_b were obtained using the subroutine PDRYS with the FTI option, and the value of Δt was also set to 10 min. The typical vial and formulation are the same as those in Table 2. The results are listed in Table 3, columns 2 and 3.

Prior to performing parameter estimation, in order to mimic actual experimental scenarios, the values of M_{ti} or T_{bi} in the second and the third columns of Tables 2 or 3 were simulated using perturbed errors at each data point, as given by the following equation:

$$Y_{ij} = Y(t,\theta) + \in_{ij},\ i = 1,M,\ j = 1,N \qquad (10)$$

where i is an index indicating the data-point number; j is an index indicating the replicate number for each data point; M is the total number of data points; N is the total number of replicates to be simulated, which was chosen to be equal to 2 in this paper, as will be discussed later; Y_{ij} is the simulated dependent variable representing either M_{ti} or T_{bi}; θ indicates the parameters of the dried-layer resistance in Eq. 1; $\in_{ij}$ symbolizes the simulated errors at data point. The errors were generated using the Monte Carlo method (Metzler, 1981; Metzler and Tong, 1981; Kalos and Whitlock, 1986), of which a random number generator was used to obtain the simulated errors. To perform the random number generation, a FORTRAN subroutine provided by Carnahan et al. (1969, p. 549) was used to obtain a pair of uniformly distributed random numbers (x_1,x_2) between 0 and 1. This procedure was performed for each data point. The resulting

Table 3
Hypothetical and estimated values of M_t and T_b as a function of time, with different vial heat transfer coefficients, KC and KP

(1) Time (min)	(2) M_{ti} (g)	(3) T_{bi} (K)	(4) $\hat{M}_t$ (g)	(5) $\hat{M}_t$ (g)	(6) $\hat{T}_b$ (K)	(7) $\hat{T}_b$ (K)	KC	KD
240	0.92458	251.759	0.92419	0.92096	251.422	251.181	2.64×10^{-4}	3.64
240	0.79408	249.741	0.79504	0.79198	249.518	249.290	1.32×10^{-4}	3.64
240	0.73262	248.676	0.73366	0.73142	248.513	248.306	1.32×10^{-4}	7.28
240	0.64104	246.949	0.64176	0.64132	246.871	246.725	0.66×10^{-4}	7.28
240	0.54707	245.014	0.54717	0.54878	244.996	244.960	0.66×10^{-4}	14.56
240	0.48428	243.644	0.48396	0.48671	243.638	243.704	0.33×10^{-4}	14.56
240	1.11073	254.138	1.10509	1.10600	253.697	253.476	5.28×10^{-4}	3.64
240	1.13179	254.376	1.12528	1.12699	253.928	253.710	5.28×10^{-4}	1.82
240	1.25532	255.672	1.24274	1.25031	255.194	254.994	7.92×10^{-4}	1.82
240	1.02715	253.134	1.02438	1.02278	252.731	252.498	3.96×10^{-4}	3.64

All data points were taken at the same drying time of 240 min. The values of R_0, A_1, A_2, A_3, A_4, and SSQ for each trial are given by the follow parameter sets obtained, indicated by the column number:
(2) Set no. 1: 5.351, 47.67, 60.18, 43.12, 7.109, SSQ = 0.3048×10^{-2} ($W_i = 1/\hat{Y}$).
(3) Set no. 1: 5.351, 47.67, 60.18, 43.12, 7.109, SSQ = 31.28 ($W_i = 1$).
(4) Set no. 2: 8.051, 37.27, 25.37, 39.51, 8.818, SSQ = 0.3066×10^{-2} ($W_i = 1/\hat{Y}$).
(5) Set no. 3: 7.032, 98.82, 68.30, 35.63, 10.75, SSQ = 0.3152×10^{-2} ($W_i = 1/\hat{Y}$)).
(6) Set no. 4: 3.271, 62.53, 49.46, 32.68, 6.522, SSQ = 29.96 ($W_i = 1$).
(7) Set no. 5: 4.705, 35.29, 35.79, 33.86, 4.835, SSQ = 31.29 ($W_i = 1$).
Note: The hypothetical experimental conditions used are the same as those in Table 2.

values of the (x_1,x_2) pairs are: (0.73275,0.53517), (0.61624,0.88095), (0.73954,0.50866), (0.39610,0.79866), (0.22704,0.17430), (0.00238,0.44562), (0.65229,0.90316), (0.54836,0.16167), (0.03481,0.75386), and (0.20981,0.47415). If the experimental error of the dependent variable follows normal distribution, the equations described by Box and Muller (1958) can be subsequently used to convert the (x_1,x_2) pair to a pair with a normal distribution (with mean zero and unit standard deviation). With a simple modification of the equations by Box and Muller, this pair can be converted to a normally distributed (Y_1,Y_2) pair, with the mean μ and the standard deviation σ, denoted as $N(\mu,\sigma)$. The resulting equations are given below:

$$Y_1 = \mu + \sigma[-2\ln(x_1)]^{1/2}\cos(2\pi x_2) \quad (11)$$

$$Y_2 = \mu + \sigma[-2\ln(x_1)]^{1/2}\sin(2\pi x_2) \quad (12)$$

where μ is equal to $Y(t,\theta)$ in Eq. 10. For M_t, σ was set to be 1% of M_{ti}, whereas for T_b, σ was set to be 1 K. The resulting values of (Y_1,Y_2) pairs generated using Eq. 11 and 12 are listed in Table 4. Thus, for each time point, two replicates were generated, with a total of 20 data points for each set of input data, in either Table 2 or 3. Since the errors for M_t were generated based on 1% of the standard deviation, the weight factor $W_i = 1/\hat{Y}$ was chosen, as described by the discussions following Eq. 9. Likewise, the weight factor $W_i = 1$ was chosen for temperature T_b. The results of parameter estimations using the computation schemes depicted in Fig. 3 are presented in Table 2 and Table 3. The values presented in columns 4 and 5 in Table 2 or 3 are the predicted values of M_t, denoted as $\hat{M}_t$, after a successful convergence of the computations with appropriate initial guesses of the parameters. These columns represent the cases with a typically low and a typically high SSQ, respectively. It can be seen that the predicted $\hat{M}_t$ values in column 4 of Table 2 or 3 are very close to the M_{ti} values in column 2, whereas those in column 5 only slightly differ from those in column 2. The predicted values of T_b, denoted as $\hat{T}_b$, after a successful convergence of the computations with appropriate initial guesses of the parameters, are presented in columns 6 and 7 in Table 2 or 3. These columns represent the cases with a typically low and a typically high SSQ, respectively. It can be seen that the values in column 6 are very close to those in column 3, whereas those in column 7 only slightly differ from those in column 3. These results indicate that the parameters obtained in Tables 2 and 3, with a typically low SSQ, are able to give a close prediction of the input data M_{ti} or T_{bi}.

Table 4
The resulting values of (Y_1, Y_2) pairs generated for M_t and T_b for each data point in Tables 2 and 3

For Table 2 Time (min)	M_t (Y_1)	M_t (Y_2)	T_b (Y_1)	T_b (Y_2)
60	0.25157	0.25308	247.96257	248.559
120	0.49108	0.48430	250.95232	249.562
180	0.70430	0.70951	250.37833	251.112
240	0.92837	0.91258	252.16866	250.461
300	1.14327	1.15169	252.96154	253.704
360	1.29669	1.35620	249.19326	253.633
420	1.55604	1.53617	253.44251	252.156
480	1.75630	1.76248	253.42063	253.775
540	1.94792	1.89627	253.02576	250.372
600	2.10873	2.15229	251.30902	253.339
For Table 3 Time (min)	**M_t (Y_1)**	**M_t (Y_2)**	**T_b (Y_1)**	**T_b (Y_2)**
240	0.91747	0.92298	250.990	251.586
240	0.79981	0.78877	250.462	249.072
240	0.72694	0.73231	247.900	248.634
240	0.64367	0.63272	247.359	245.652
240	0.55138	0.55544	245.803	246.545
240	0.46842	0.48992	240.369	244.809
240	1.11915	1.10486	254.897	253.610
240	1.13833	1.14233	254.954	255.308
240	1.25611	1.22280	255.735	253.081
240	1.00924	1.03008	251.390	253.420

The accuracy of the normalized dried-layer resistance is assessed here using the obtained parameter sets in Tables 2 and 3. The values of $\hat{R}_p$, indicated by Eq. 1, for the parameter sets obtained in Table 2 and 3 were computed using the primary drying subroutine PDRYS with the FTI option, and presented in Fig. 4 and Fig. 5, respectively. It should be emphasized that it is not appropriate to use Eq. 1 to directly compute $\hat{R}_p$ for this assessment, since $\hat{R}_p$ is defined as a function of the temperature at the moving sur-

face of the frozen layer T_a in this paper, which is a variable over the entire drying period. Fig. 4 shows that the three parameter sets, sets no. 2, 3 and 4, give fairly close prediction of $\hat{R}_p$ over the entire time period simulated. Set no. 5, which represents a parameter set with a typically high SSQ, gives a higher deviation in predicting $\hat{R}_p$. By comparing Fig. 5 with Fig. 4, it shows that the parameter sets in Fig. 5 give a relatively higher deviation from the theoretical $\hat{R}_p$ values than that in Fig. 4. As shown in Fig. 5, sets no. 2, 3 and 4 give a closer prediction than sets no. 5 which represents the case with a typically higher SSQ. The results presented in Fig. 4 and 5 indicate that the parameter set with a typically low SSQ is able to give a close prediction of $\hat{R}_p$ with the perturbed errors investigated. For the parameter set with a typically high SSQ, such as set no. 5, an interesting phenomenon is observed by comparing Fig. 4 with the numerical values in Table 2, or Fig. 5 with the numerical values in Table 3. It

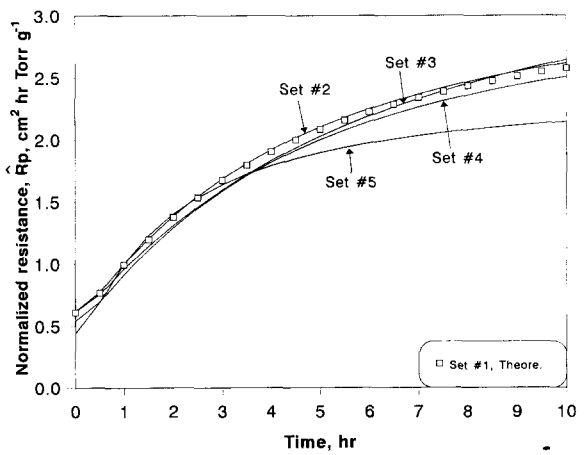

Fig. 4. Comparison of dried-layer resistances for various estimated parameter sets in Table 2. These parameter were obtained after successful convergence using appropriate initial guesses of the parameters, with the following short-hand codes: (1) TPL: typically low SSQ; and (2) TPH: typically high SSQ. Set no. 1, theoretical parameters: 5.351, 47.67, 60.18, 43.12, 7.109. Set no. 2: time variation, simulated M_t data, parameters with TPL: 6.574, 55.56, 42.63, 39.00, 8.748. Set no. 3: time variation, simulated M_t data, parameters with TPH: 5.402, 44.38, 9.988, 23.98, 7.109. Set no. 4: time variation, simulated T_b data, parameters with TPL: 3.484, 35.11, 78.11, 47.39, 4.376. Set no. 5: time variation, simulated T_b data, parameters with TPH: 2.148, 37.33, 62.72, 35.05, 0.6187.

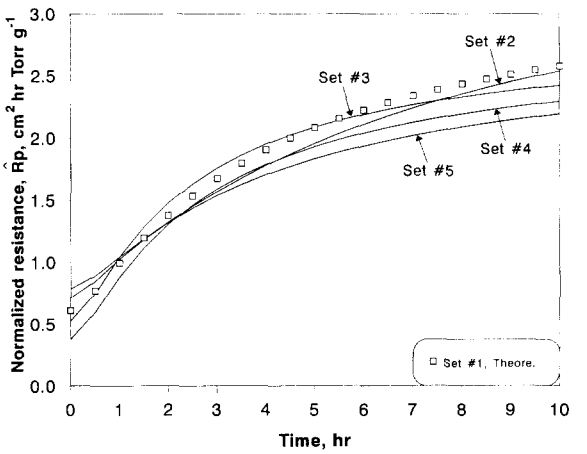

Fig. 5. Comparison of dried-layer resistances for various estimated parameters in Table 3. These parameter were obtained after successful convergence using appropriate initial guesses of the parameters, with the following short-hand codes: (1) TPL: typically low SSQ; and (2) TPH: typically high SSQ. Set no. 1, theoretical: 5.351, 47.67, 60.18, 43.12, 7.109. Set no. 2: K_y variation, simulated M_t data, parameters with TPL: 8.051, 37.27, 25.37, 39.51, 8.818. Set no. 3: K_y variation, simulated M_t data, parameters with TPH: 7.032, 98.82, 68.30, 35.63, 10.75. Set no. 4: K_y variation, simulated T_b data, parameters with TPL: 3.271, 62.53, 49.46, 32.68, 6.522. Set no. 5: K_y variation, simulated T_b data, parameters with TPH: 4.705, 35.29, 35.79, 33.86, 4.835.

shows that the deviation between the predicted M_t or T_b and the theoretical one is much smaller than the deviation between the predicted $\hat{R}_p$ and the theoretical one. In fact, the values in column 7 of Table 2 or 3 are fairly close to those in column 3 of either table.

4. Conclusions

The proposed approach is robust for estimation of the dried-layer mass transfer coefficients during primary drying using experimental data obtained from various experimental conditions, including the non-isothermal conditions. The numerical exercises demonstrate that both the cumulative mass of sublimation M_t and the temperature profile at the bottom center of the frozen layer T_b can be successfully used as the input data to obtain desired mass transfer coefficients. In fact, the temperature profile at any specific

location along the axis of the cylindrical frozen layer may also be used. The experimental efforts may be minimized by the proposed approach in two ways. First, since the temperature profile at a location in the frozen layer can be easily monitored without a major alteration of the freeze dryer, the proposed approach can considerably minimize experimental efforts. Second, it may also be possible to minimize experimental efforts without alteration of the freeze dryer by using vials with different heat transfer coefficients. This strategy, however, needs to be substantiated using an actual experiment. The FORTRAN programs and documentation are available upon request from W. Kuu, where the documentation contains all detailed mathematical equations and computational steps.

5. Glossary

Symbol	Meaning
A_1, A_2, A_3, A_4	mass transfer coefficients, used in Eq. 1
A_p	cross-sectional area of the product in the vial, in cm^2
ASV	shelf area per vial, in cm^2
ATV	tray area per vial, in cm^2
A_v	vial area (calculated based on the outside diameter), in cm^2
d	inside diameter of the vial, in cm
KC,KD	constants associated with vial heat transfer coefficient
K_I	effective thermal conductivity of the frozen layer
KP	constant associated with vial heat transfer coefficient
K_S	heat transfer coefficient
KTC,KTP,KTD	constants
K_{tr}	tray heat transfer coefficient
K_v	vial heat transfer coefficient
ℓ_m	maximum thickness of the frozen layer, in cm
$M_t(t)$	cumulative mass of sublimation at time t, in g
$\hat{M}_t(t)$	estimated cumulative mass of sublimation at time t, in g
$M_{ti}(t)$	simulated cumulative mass of sublimation, in g; used to mimic the experimentally determined value
ℓ	thickness of the dried layer at any time, in cm
ℓ_m	maximum thickness of the frozen layer, in cm
$\dot{m}$	sublimation rate, in g/h
$\dot{m}_{avg}$	average rate of sublimation, in g/h
$N(\mu,\sigma)$	normal distribution, with a mean of μ and a standard deviation of σ
NS	number of drying stage used for computations
P_0	equilibrium vapor pressure of the subliming ice, in mmHg
P_c	chamber pressure, in mmHg
P_v	pressure in the vial, in mmHg
R_0	dried-layer mass transfer coefficient, used in Eq. 1
R_p	dried-layer resistance, in (Torr h g^{-1})
$\hat{R}_p$	area normalized dried-layer resistance, in (cm^2 Torr h g^{-1})
R_s	stopper resistance
S_0, S_1	stopper mass transfer constants
SSQ	sum of squares
T_a	temperature at the moving surface of the frozen solution, in K
T_b	temperature at the bottom center of the frozen layer, in K
$\hat{T}_b$	estimated temperature at the bottom center of the frozen layer, in K
T_{bi}	simulated temperature at the bottom center of the frozen layer, in K; used to mimic the experimentally determined value
T_f	temperature of the cooling fluid in the freeze dryer, in K
T_s	shelf temperature, in K
T_t	surface temperature of the tray, in K

W_i	weighting factor used in Eq. 9
(x_1,x_2)	a pair of uniformly distributed random numbers
(Y_1,Y_2)	a pair of normally distributed dependent variable Y, as given by Eq. 11 and 12
Y_i	observed dependent variable, representing either M_{ti} or T_{bi}
$\hat{Y}$	estimated dependent variable, representing either $\hat{M}_t$ or $\hat{T}_b$
ϵ	porosity or volume fraction of water in the frozen layer
$\in_{ij}$	error of the dependent variable of either M_{ti} or T_{bi}, used in Eq. 10
θ	parameter of the dried layer resistance in Eq. 1, used in Eq. 10
μ	mean of the dependent variable of either M_t or T_b.
σ	standard deviation of the dependent variable of either M_t or T_b
ρ_1	density of ice, in g/cm^3

References

Box, G.E.P. and Muller, M.E., A note on the generation of random normal deviates. *Ann. Math. Stat.*, 29 (1958) 610–611.

Carnahan, B., Luther H.A. and Wilkes J.O., *Applied Numerical Methods*, Wiley, New York, 1969, p. 545.

Dyer, D.F. and Sunderland, J.E., Heat and mass transfer mechanism in sublimation dehydration. *J. Heat Transfer*, 90 (1968) 379.

Himmelblau, D.M., *Applied Nonlinear Programming*, McGraw-Hill, New, York, 1972.

Ho, N.F.H. and Roseman, T.J., Lyophilization of pharmaceutical injections: Theoretical physical model. *J. Pharm. Sci.*, 68 (1979) 1170–1174.

Jennings, T.A., Discussion of primary drying during lyophilization. *J. Parenter. Sci. Technol.*, 42 (1988) 118–121.

Kalos, M.H. and Whitlock, P.A., *Monte Carlo Methods, Vol. I: Basics*, Wiley, New York, 1986.

Karel, M., Heat and mass transfer in freeze-drying. In Goldblithm, S.A., Rey, L. and Rothmayr, W.W. (Eds), *Freeze-drying and Advanced Food Technology*, Academic Press, New York, 1975, pp. 177–202.

Kuu, W.Y., Determination of residence-time distribution in i.v. tubing of in-line drug delivery system using deconvolution technique. *Int. J. Pharm.*, 88 (1992) 369–378.

Kuu, W.Y., Wood, R.W. and Roseman, T.J., Factors influencing the kinetics of solute release. In Kydonieus, A. (Ed.), *Treatise on Controlled Drug Delivery*, Ch. 2, Dekker, New York, 1992, pp. 37–154.

Lombrana, J.I. and Diaz, J.M., Heat programming to improve efficiency in a batch freeze-drier. *Chem. Eng. J.*, 35 (1987) B23–B30.

Mellor, J.D. *Fundamentals of Freeze-drying*, Academic Press, New York, 1978.

Metzler, C.M., Statistical properties of kinetic estimates. In Endrenyi L. (Ed.), *Kinetic Data Analysis*, Plenum Press, New York, 1981, pp. 25–37.

Metzler, C.M. and Tong, D.D.M., Computational problems of compartment models with Michaelis-Menten type elimination. *J. Pharm. Sci.*, 70, 733–737 (1981).

Millman, M.J., Liapis, A.I. and Marchello, J.M., An analysis of the lyophilization process using a sorption-sublimation model and various operational policies. *AIChE J.*, 31 (1985) 1594–1604.

Nail, S.L. The effect of pressure on the heat transfer in the freeze-drying of parenteral solutions. *J. Parenter. Drug. Assoc.*, 34 (1980) 358.

Pikal, M.J., Use of laboratory data in freeze drying process design: heat and mass transfer coefficients and computer simulation of freeze drying. *J. Parenter. Sci. Technol.*, 39 (1985) 115–138.

Pikal, M.J., Roy, M.L. and Shah S., Mass and heat transfer in vial freeze-drying of pharmaceuticals: role of the vial. *J. Pharm. Sci.*, 73 (1984) 1224–1237.

Pikal, M.J., Shah, S., Senior, D. and Lang, J.E., Physical chemistry of freeze drying: Measurement of sublimation rates for frozen aqueous solutions by a microbalance technique. *J. Pharm. Sci.*, 72 (1983) 635–650.

Powell, M.D.J., A method for minimizing a sum of squares of nonlinear functions without calculating derivatives. *Comput. J.*, 7 (1965) 303–307.

Rohsenow, W.M., Hartnett, J.P. and Ganić, E.N., *Handbook of Heat Transfer Fundamentals*, McGraw-Hill, New York, 1985, pp. 3–50, Table 33.